Characterization, Testing and Operation of Omega2000 Wide Field Infrared Camera

Zoltán Kovács, Ulrich Mall, Peter Bizenberger, Harald Baumeister, Hermann-Josef Röser

Max-Planck-Institut für Astronomie, Königstuhl 17 D-69117 Heidelberg, Germany

ABSTRACT

Omega2000 is the first near infrared (NIR) wide field camera installed on the 3.5 m telescope at Calar Alto which operates with a 2kx2k HAWAII-2 FPA. Each component of the camera system must suit high requirements to exploit the facilities provided by the imaging sensor. To meet these requirements was a great challenge in design and realization of the optics, the mechanical part and the electronics. The cryogenic optical system with a warm mirror baffle can produce excellent optical quality and high sensitivity over the whole 15.4x15.4 arcmin field of view. The readout electronics together with the camera control software provide multi functional data acquisition and the camera control software can perform the readout and on-line data reduction simultaneously at a high data rate. Different operational and readout modes of the data acquisition of the detector both for engineering and scientific purpose were implemented, tested and optimized and the characteristics of three HAWAII-2 detectors were also determined in their hardware and software environment. Initial astronomical observations were carried out successfully in autumn 2003.

Keywords: wide field near infrared camera, HAWAII-2 FPA

1. INTRODUCTION

After the first observations and the preliminary data reduction, the results achieved with Omega2000, a new NIR wide field camera mounted on the 3.5 m telescope at Calar Alto, seem promising. The camera uses a HAWAII-2 2kx2k HgCdTe array from Rockwell. Many requirements must be met by each component of the camera system to exploit the facilities provided by the imaging sensor. These requirements meant a great challenge in design and realization for both the optics, the mechanical parts and the electronics. First we give a brief account of the cryogenic optical system consisting of a four-lens focal reducer located in the prime focus, which can produce excellent optical quality and high sensitivity over the whole 15.4x15.4 arcmin field of view with a resolution of 0.45"/pixel. Then a concise summary follows on the mechanical design of the filter wheels and the warm mirror baffle system. We continue with a short description of the general readout electronics of Omega2000 designed for a number of different instruments, including MIDI and LUCIFER. Although the electronics contain universal functional units, they were configured to fit the peculiar requirements. We characterize the multi functional data acquisition and camera control software providing an interpreter for execution commands and a graphical interface for data visualization and parameter setting, which can perform the readout and the data saving simultaneously at a high data rate. We also discuss how the different readout modes of the data acquisition of the detector both for engineering and scientific purpose were implemented, tested and optimized and how the characteristics of three HAWAII-2 detectors were determined in their hardware and software environment. Initial astronomical observations taken in autumn 2003 are also presented.

2. OMEGA2000 DESIGN

Since the primary science goal was for Omega2000 to be a wide field imager producing high quality images with the largest feasible pixel scale, it was placed at the prime focus of the 3.5m telescope at Calar Alto. The camera was designed without reimaging optics to avoid any degradation of the image quality by the complex optical system as the field of view or the pixel scale is increased. However, for ground based IR imaging not only the photon noise from the background due to the predominant OH air-glow of the sky can be a noise source but also the thermal radiation from the warm telescope mirrors, structure and dome. The first source is only significant
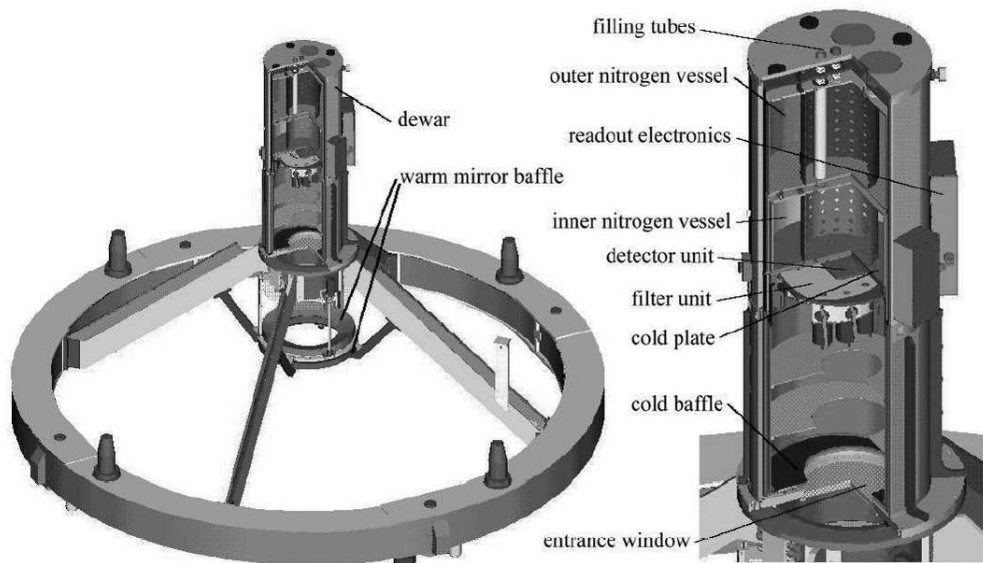
Figure 1. Omega2000 dewar mounted on front ring.

for J and H band imaging but the second one can also cause problems in K band without reimaging. As a solution, the camera is equipped with a baffle system to minimize the amount of radiation reaching the detector in K band.[1] To eliminate the background noise, the detector and the optics are enclosed in a vacuum dewar and cooled by liquid nitrogen to the operating temperature, 77 K. The dewar also contains three shields nested into each other to reduce the thermal radiation (Fig. 1). The liquid nitrogen is stored in two vessels that can be filled on the telescope through the upper side of the dewar. One of the vessels is directly connected to the inner radiation shield and the other one to the second shield. The lower end of the inner vessel also serves as a base for the cold plate of the detector unit. The baffle system of Omega2000 consists of one cold and two warm mirror baffles. The cold baffle is located inside the dewar to reduce thermal background emitted by surrounding of the telescope pupil. The position of the cold baffle is as far from the detector as possible but their distance is limited by the size of the dewar window, feasible dewar dimensions and a maximum tolerated central obscuration. The warm baffles of the camera are annual sections of an oblate ellipsoid with the edges of the cold baffle as the foci. The first baffle (diameter 750 mm) is at a fixed position and does not vignette the field of view. The second baffle has a smaller inner diameter and it is designed to vignette the entire field of view uniformly. It prevents the detector from seeing the warm surrounding of floor, which improves the S/N ratio in the K band. For J and H band observations, the baffle can be moved closer to the dewar to a position where it does not vignette at all.[2] A focal reducer is used to increase the pixel scale to 0.45"/pixel. It has four lenses made of CaF_2, fused silica (FS), BaF_2 and ZnSe with diameters between 106 and 150 mm, which are achromatic between 850 and 2500nm (Fig. 2). Each lens is fixed by a spring-loaded retainer ring in a single assembly. To achieve an excellent optical image quality and to minimize the lens diameters, the focal reducer unit is located in the dewar, as close to the detector as possible. This means it is cooled down to a temperature of about 80 K, so the most difficult task of the lens mount design was to make sure that the lenses survive cooling and at the same time achieve the tight tolerances required by the optical quality. Omega2000 contains 17 filters of 3 inch diameter for wavelengths between 0.8 and 2.4 μm and one closed blank, which are distributed over three filter wheels. The filter unit containing the wheels, the cryogenic stepper motors and the locking/cooling mechanisms is placed between the detector and the focal reducer. Each wheel, mounted on a cryogenic ball bearing, contains seven equally spaced locking positions (six for filters and one free opening) and each filter position has a 3-bit magnet arrangement for determining the selected filter by three Hall sensors.

The detector fanout board holds a Zero Insertion Force (ZIF) socket mount for the HAWAII-2 detector. The central pins of the socket and the detector are used for thermal contact, whereas the outer two rows on each side
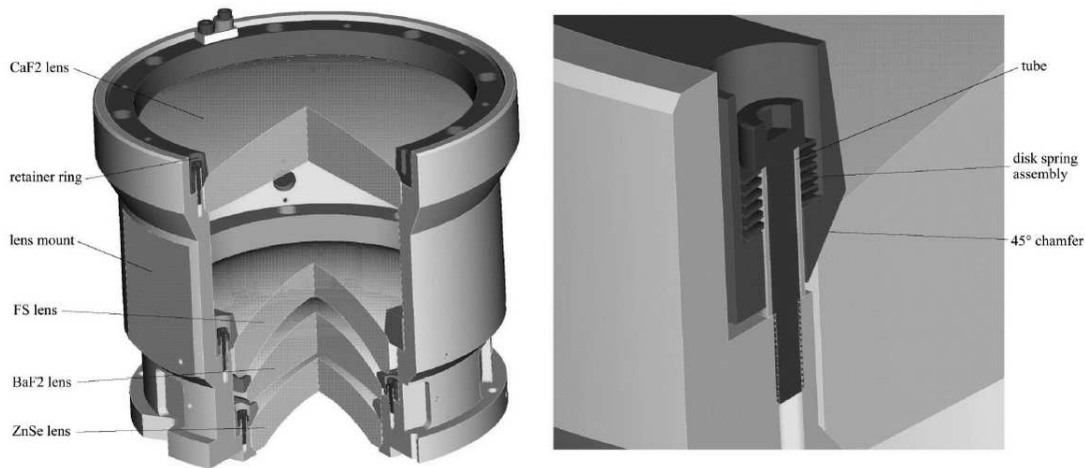
Figure 2. Four-lens focal reducer with spring loaded cryogenic lens mount.

are electrical contacts. The detector unit consists of a rigid aluminum base plate which carries the fanout board on 12 identical cylindrical supports. To cool the detector a spring-loaded cooling mechanism is used. A copper bar, which is preloaded by springs, presses an indium foil against the central detector pins.

The video outputs of the HAWAII-2 FPA go to two preamplifier boards via 16-16 channels and the amplified signals organized in four cables are sent to the readout electronics containing eight boards of AD converters, which receive the amplified video signals. A Digital Signal Processor (DSP) clocks the readout process of the chip and the timing of the data transfer through control channels and triggers the AD conversions. These tasks are implemented in the form of patterns, instruction tables and macros handled by the DSP. The patterns are sequences of control signals of the chip and the instruction tables consist of linear sequences and loops of instructions which determine the timing and repetition of these patterns. The macros for the pattern generator contain instructions for more general purpose such as running instruction tables in the DSP memory or controlling the DSP itself. The digitized video outputs from two BUSLINK cards, via FDDI cables, arrive at a signal converter which transforms them to a proper data format for a Sun workstation. The DSP is controlled by a microprocessor which communicates the IR control software running on the workstation.

The data acquisition and control software used for Omega2000 is Generic InfraRed camera Software (GEIRS) developed for the general readout electronics. The software is able to sustain a high data transfer rate continuously, have data visualization control and save the data in time to hard disks. These tasks have been implemented by efficient organization of shared data buffers and parallel processing with optimal usage of the multiprocessor capabilities. Besides the command line prompt, the control software has a graphical user interface with control panels and a display for the video output. The parameters of the readout process can be set and modified in the control panels. Each readout mode is implemented in different instruction tables, which the control software can load and send to the DSP. The parameter files of GEIRS contain these instruction tables, different clock and control patterns for the 1 and 8 output modes and macros calling the instruction tables in different output, readout and idle/non-idle modes. The control software stores the parameters in variables, such as the integration time, the repetition number of readout, the actual readout and output mode or the filter and baffle positions. During the initialization process the clock and control patterns, the instruction tables and the macros required for the actual output and readout modes are sent to the DSP by the software. If a parameter is changed via the control panel, the software reinitializes the electronics and sends the new instruction tables and macros to the readout electronics before starting any readout process. The readout frames are stored in a memory buffer and saved interactively or by GEIRS commands. The commands of the control software can be organized batches, i.e., in predefined series of readout commands with given integration times, repetition counter, and other commands to synchronize the different steps or move the telescope. We used the environment of GEIRS to test and characterize different HAWAII-2 detectors but the observations were carried out with MIDAS utilities controlling
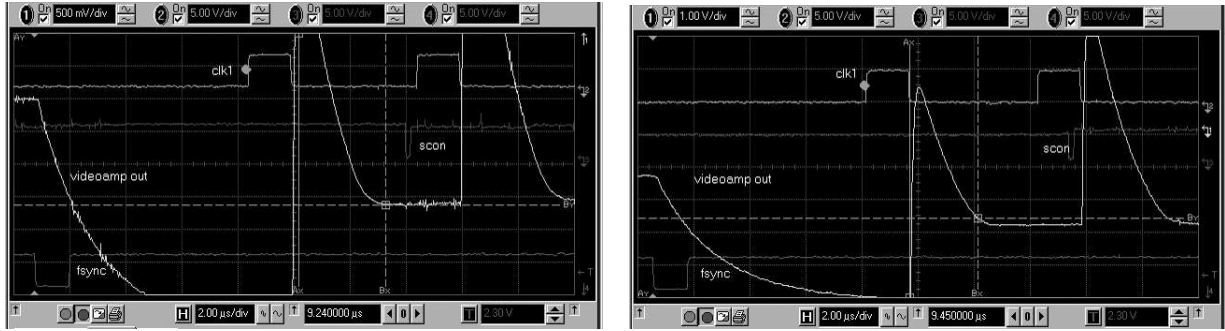
Figure 3. The normal triggering (left panel) and triggering with delay (right panel) of the video signal conversion.

GEIRS itself.

3. DETECTOR READOUT

Omega2000 was designed for background-limited operation, which determined the requirements for the optimal camera readout process. In order to avoid the background excess, we had to achieve as fast operation of the detector as possible while keeping the readout noise under the photon shot noise of the background. The eight-output unshuffled mode in the three output modes available for HAWAII-2 chip was applied because it has the highest speed. Although stripe patterns due to systematic effects could be eliminated in the shuffled output mode, they do not cause any problem because of the dominating background noise. Besides the choice of the output mode with the fastest data transfer, the duration a pixel readout cycle was minimized by the proper timing of the clock and controlling signals and different solutions of the readout modes of the full array was also implemented by organizing the pixel readout cycles in different ways.

The main purpose for optimizing the pixel readout cycle is to increase the sampling frequency of the video signal to an upper limit beyond which the sampled signal was distorted due to the interference and the transient behavior of the circuit components. The upper limit of the sampling and clocking frequency is therefore determined by the transient time of the video signal. After the video signal is pulled up, it cannot be sampled until it has reached its stable value, which takes about 400 ns with an optimal dynamical range adjusted with 1V reset voltage and 3.2 V biasgate voltage. The readout cycle time of one pixel is minimum 600 ns corresponding to a clock frequency of 166 kHz. Since the readout cycle of a pixel starts at the rising edge of the clock signal but the video signal is pulled up only at the falling edge, there is a possibility to increase the clocking frequency. We can use not only the time period of the low state of the clock signal (between the falling and rising edges) but also the one of the high state of the clock signal (between the rising and falling edges) in the next cycle to cover the whole transient time of the video output (Fig.3). By applying a shorter low state of the clock signal, the next readout cycle will start earlier and the video output can be sampled before the falling edge of the clock signal in the next readout cycle and the result will be a readout cycle with shorter time period. Another possibility is to decrease the transient time of the video signal itself. If the column bus is not reset to celldrain while no readout the jump of the video signal due to the pulling up is lowered, which decreases the transient time to 200 ns. This solution allowed us to raise the clock frequency to 250 kHz. Although a stable video signal is sampled with all the methods, we used a pixel readout time of 600 ns (166 kHz) because ramps appeared at the edge of the frames taken with higher clock frequency (see the next section).

Since a line reset is implemented for the HAWAII-2 chip, we can apply different schemes of Correlated Double Sampling (CDS). The traditional readout cycle with CDS consists of a full array reset, a readout of the reset level, and another one of the signal value after integration. The resulting frame is provided by the subtraction of the reset level from the integrated signal. In this scheme the array is clocked through three times for the resetting (1024 line reset pulse per quadrant) and the two readouts (Fig. 3). It is more efficient to combine the reset and the first readout of the array. Each line reset can be followed by the readout of the reset level (1024 times "start of conversion" (SCON) pulse per line) and a second readout of the video signal after integration.
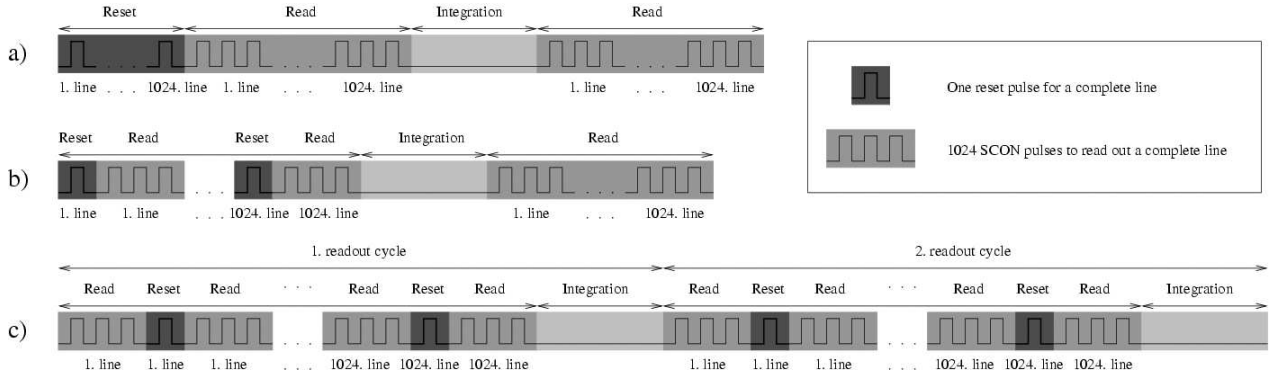
Figure 4. Different readout modes with CDS implemented for HAWAII-2. a) traditional Correlated Double Sampling. b) Correlated Double Sampling with fast reset c) line interlaced mode.

In this case, the full array is clocked through only two times for the reset with readout and the second readout. It is possible to extend this "fast reset" schema to the second readout too in such a way that the readout of the integrated signal in each line is followed by a line reset and a readout of the reset values in that line. As a result, a complete frame is reset and its reset level is read out for the next cycle while the array is clocked line by line to obtain the integrated signal in the actual cycle. This method of interlacing the neighboring readout cycles of lines is the most effective solution for CDS because each line is reset and the bias values are read immediately after reading the integrated pixel values. The CDS with fast reset waits until the video signals in the whole array have been read before resetting the unit cells in the next cycle. To obtain just a single image the CDS with fast reset takes the same time as the line interlaced mode, but for a sequence of many repeats, the latter is much quicker. We also implemented other readout modes, such as the readout of a single pixel at an arbitrary position per channel or the reset level readout for testing purpose. All the different schemes of CDS were developed for the observations but the choice of the applied readout mode, of course, depends on the performance of the camera with it.

4. PERFORMANCE OF THE CAMERA

The performance of Omega2000 was tested extensively at MPIA and during several commissioning runs at Calar Alto. Most of the problems related to the operation of the mechanical part, the optics and the readout electronics with the detectors could be solved or their consequences were mitigated insomuch they did not degrade the performance of the camera.

The optical quality produced by the wide field imager completely fulfills the requirements. To determine its optical distortion, distances between a star at the center and all the other objects in the field of view was calculated both from the measured positions and directly from the differences of the RA and DEC positions. The ratio of the two distance determinations was fitted as a function of distance from the field center. The center to corner image distortion was measured to 0.12" for the maximum distance of 600", which is less than one pixel (Fig. 5). Nevertheless, we had seen scattered light and reflections which were attributed to the shining aluminum surface of the optics mount. The largest accessible areas were covered to eliminate them but the bevels defining the lens positions could not be painted and they are still reflecting surfaces. There are also reflections between the filter surface and the outermost lens producing almost in-focus images. This would explain the "ghost images" of the primary mirror in the flatfields (Fig. 5). Although they appeared in the raw science frames, we could subtract them properly in the corrected images and their residuals were negligible to the background.

MPIA had the opportunity to test the operation of Omega2000 camera with three different HAWAII-2 focal plane arrays with the serial number #37, #48 and #77. Therefore the dark current statistics, readout noise properties, linearity tests and the distributions of their quantum efficiency could be compared for the different sensors to give a more comprehensive view on the performance of this detector family.
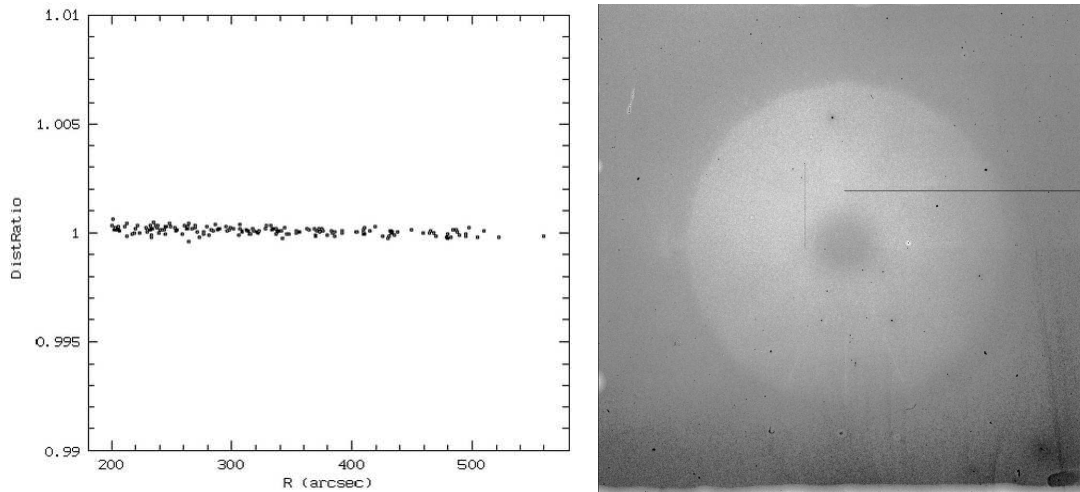
Figure 5. Left panel: distortion ratio vs. distance diagram. Right panel: a flatfield frame with the reflection of the primary mirror (FPA #48).

Dark frames were taken with different integration times from the minimal frame readout times up to 2000 s by using the blank disk inserted in the filter wheel. The dark current of HAWAII-2 detectors is only about 0.02 e^-/s at 77 K, which means that the median value of the dark signal with the integration time of 2000 s is expected to be 40 e^-.[3] However, the medians of the dark frames of each FPA taken with the same integration time were normally measured to 200 e^- (about 50 ADU), i.e., the dark current was completely dominated by other noise sources. The typical noise features were periodic noise patterns due to the readout electronics and the glowing of the output transistors. The glowing caused only a small excess on the right wing of dark frame histograms and did not change their mean values, which were determined by the noise of the external amplifiers.
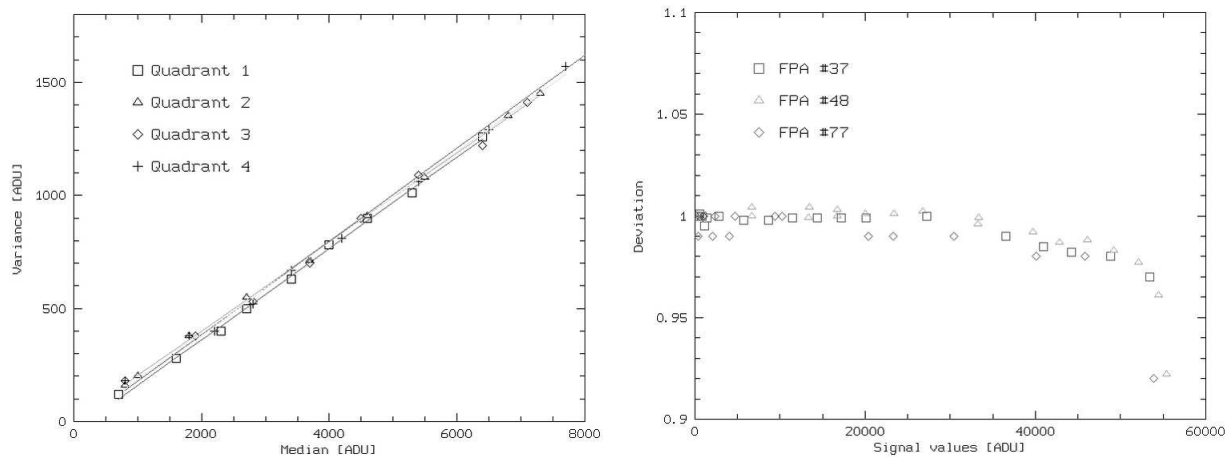

Figure 6. Left panel: photon transfer curves for each quadrant of FPA #37. Right panel: linearity tests of different HAWAII-2 detectors.

We used flatfield images taken with constant illumination through a narrow band filter (NB1083) with different exposure times to determine the readout nose and the gain of the detectors. The median and the variance of the pixel values were measured in each channels of the arrays and they were averaged for each quadrant (Fig. 6). The photon transfer curves of the three arrays had very similar characteristics. Their tangents providing the

gains of the detectors were between 4.2-5.2 e^-/ADU and their values at zero gave a readout noise of 10 e^- on the average, as expected.[4]
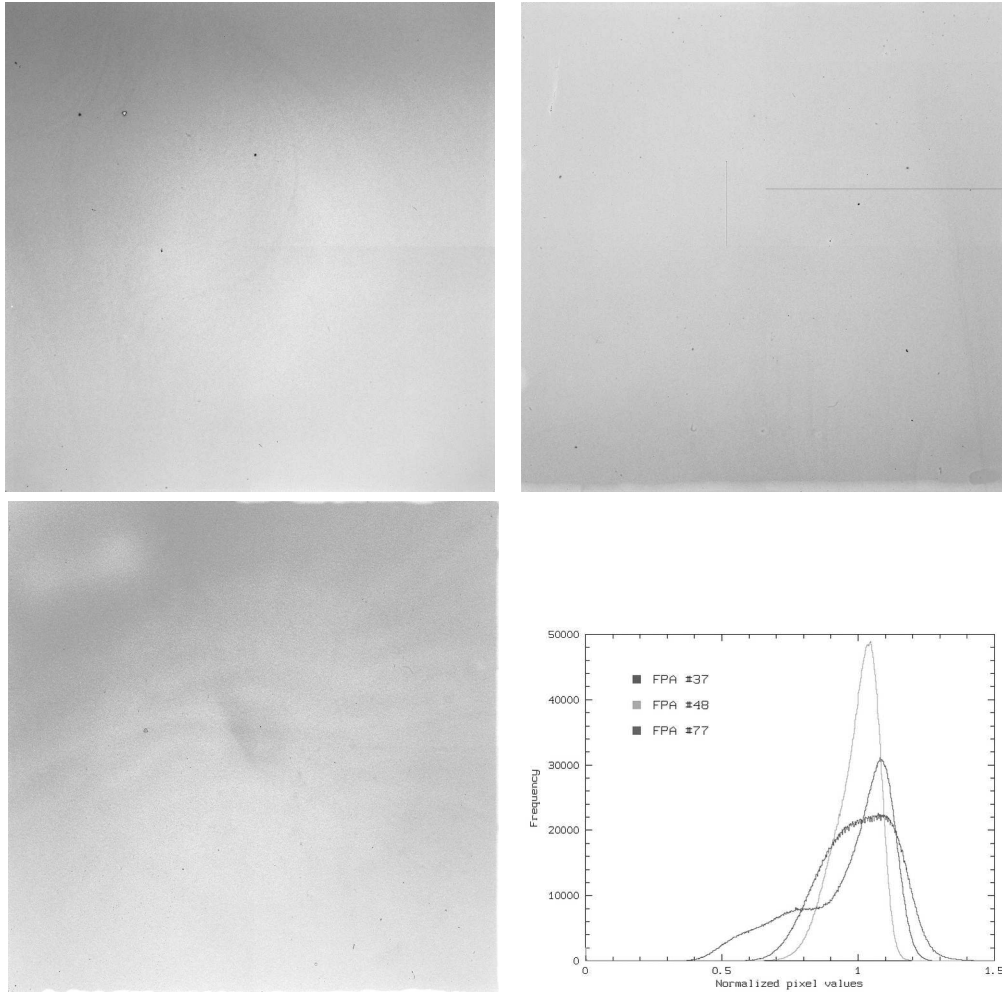

Figure 7. Flatfield images of FPA #37 (upper-left), #48 (upper-right) #77 (lower-left) and their histograms (lower-right).

The linearity of the detectors was measured by taking flatfields with different integration times and constant illumination through a narrow band filter (NB1083). Since the dark current of the HAWAII-2 chips is very low and the maximal exposure time was 2000 s, the dark current contribution had a negligible effect on the measured signal. We measured the non linearity of the signal with increasing exposure time, i.e., the deviation of the signal value from the linearly scaled values with time. All of the detectors #37, #48 and #77 were linear within 1% of the signal up to about 40000 ADU, which means the full well capacity of each FPA is about 200000 e^- (Fig. 6).

In order to characterize the quantum efficiency of the different detectors, flatfield images were taken in K band and normalized with their median. When the histograms of the flatfield frames are compared with each other, the difference between the distribution of the quantum efficiency of the imagers can be established: the narrow peak of the histogram belonging to FPA #48 shows that this chip has the most uniform distribution of the quantum efficiency. The left wing of the histogram of FPA #37 indicates a higher non-uniformity in its upper left quadrant while the broad, less pronounced bump in the histogram of FPA #77 is caused by a global variation of the quantum efficiency in the whole array. The flat field images illustrate well these different distributions (Fig. 7).
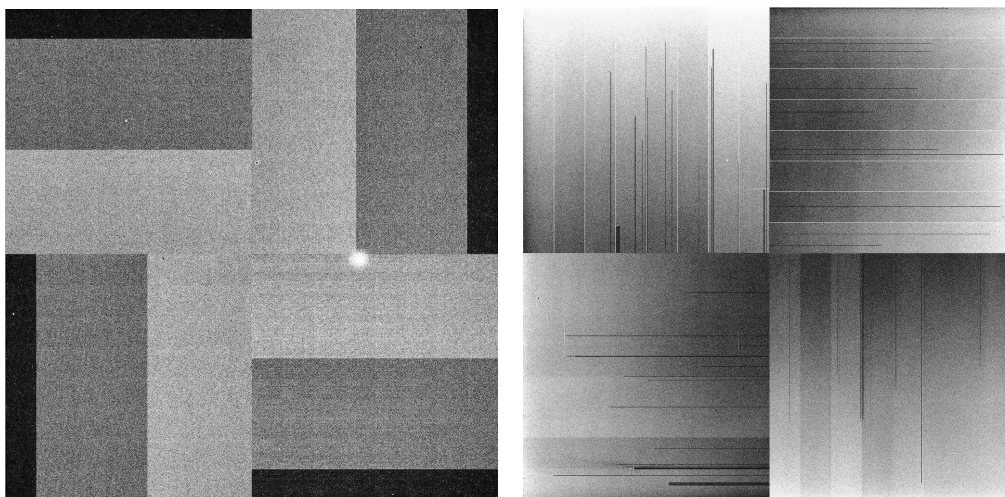
Figure 8. Dark frames taken with FPA #37 in CDS mode with fast reset (left) and in traditional CDS mode (right).

Besides the dark current subtraction, the thermal frames of the detectors also served to separate bad pixels from healthy ones. We made a root mean square map of the deviation of each pixel in a stack of dark frames taken with different integration times from the values in the scaled thermal frames. Since a thermal frame is a result of a linear fitting, an RMS map contains the scattering of the signal values around the scaled fit. Its histogram at high values represents the pixels for which the linear fitting failed because of their highly non-linear response, so the map helps to discriminate the bad pixels from the hot and the normal ones. Besides the individual hot pixels, bad pixels could be found in groups in each array and the FPA #48 had also bad colums. However, the bad pixel masks created by using this method contained about 1000, 3600 and 5000 bad pixels for FPA #37, #48 and #77, respectively. This means more than 99.8% of the pixels could be corrected by dark current subtraction and flatfielding for all the three detectors.

All the implemented CDS readout modes were tested with clock frequencies between 150 and 250 kHz by checking the quality of their result images. The noise statistics of the frames taken with different clock rates did not change dramatically but some artifacts degrading the image quality appeared at higher clock frequencies. A typical problem was that the different groups of channels had different offsets in the frames of low signal level taken in CDS mode with fast reset (Fig. 8). With slow reset or in line interlaced mode, only a gradient or a ramp in the pixel values appeared in the quadrants but this artifact had a non-linear behavior, i.e., it did not scale with the average signal level. We used slower clock rates down to 150 kHz but the ramps could not be eliminated. This phenomenon might be caused by some unknown coupling problem between the multiplexer of the detector and the data bus of the readout electronics. Nevertheless, we did not observe any similar feature in the images produced with the FPS #48 in the traditional CDS with the clocking frequency of 166 kHz. The last year this specimen was used during observations and Omega2000 could provide data of good quality at clear nights. The last session this year, the camera operated with the FPA #77 in one output mode because the ramps were less steeper in this mode. The ramps could be flatfielded out and the preliminary results of the data reduction were satisfying but the slower output mode increased the dead time of the dithering.

Although bright stars can saturate the detector, resetting of the full array prevents this high excess in the pixel values from causing any residual image effects in the following image of the dithering. Nevertheless, the saturated pixels generate a crosstalk between the data transfer lines of the different channels of the quadrant in which they are situated. The data lines of the channels are organized in parallel and there might be an interference between the data lines transferring the high video signal and the neighbour ones. As a result of this crosstalk, a series of spots with the distances of 128 pixels from each other appeares in the whole quadrant, corresponding to each channel. The average values of the spots were lower than the background signal and their difference was few percent, which is large enough to degrade the photometric correctness at the place they are

situated. These spots could not be measured in the raw images but they were well discernible in the reduced frames (Fig. 9). This effect was a general feature of the operation of all the HAWAII-2 detectors we tested and should be considered for the choice of pointing positions in any field of next observations.
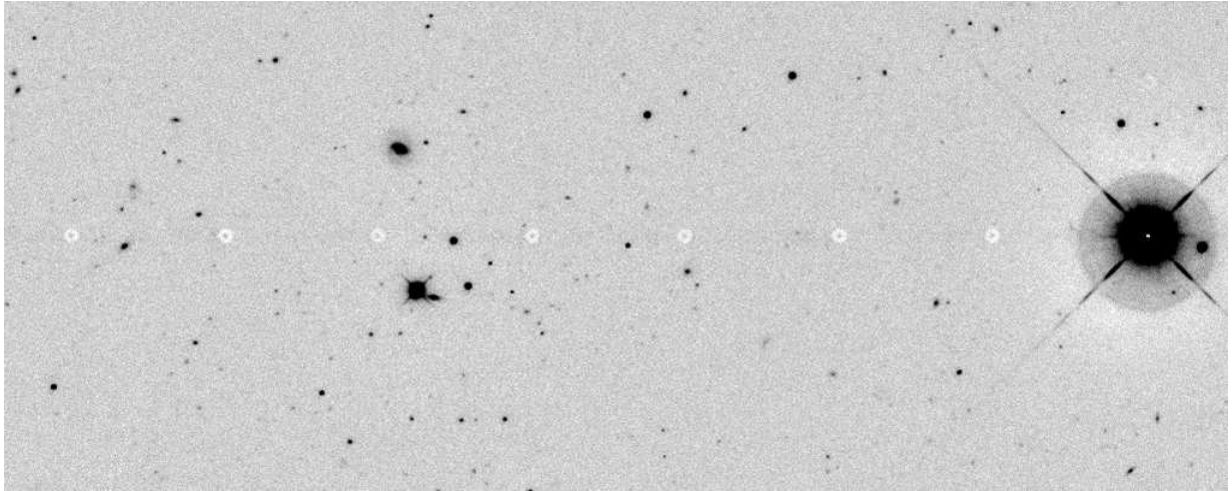

Figure 9. A series of spots caused by the cross talk during transferring the high signal values of the saturated pixels.

Finally we show two images as results of the preliminary data reduction to demonstrate the operability of Omega2000, the new wide field imager (Fig. 10). The frames were taken in H band and with a narrow band filter with a central wavelength of 1200 nm and a bandwidth of 90 nm (the short end of the J band). The field of view of summed images is still about 15x15 arcmin while the FWHM of the PSF is 1.1" in the H band image and 0.9" in the narrow band image,. The exposure time was 3000 s for both frames and the limiting magnitudes in the Vega system were measured to 21.4 mag in H band and 22.4 mag for the narrow band filter, respectively.
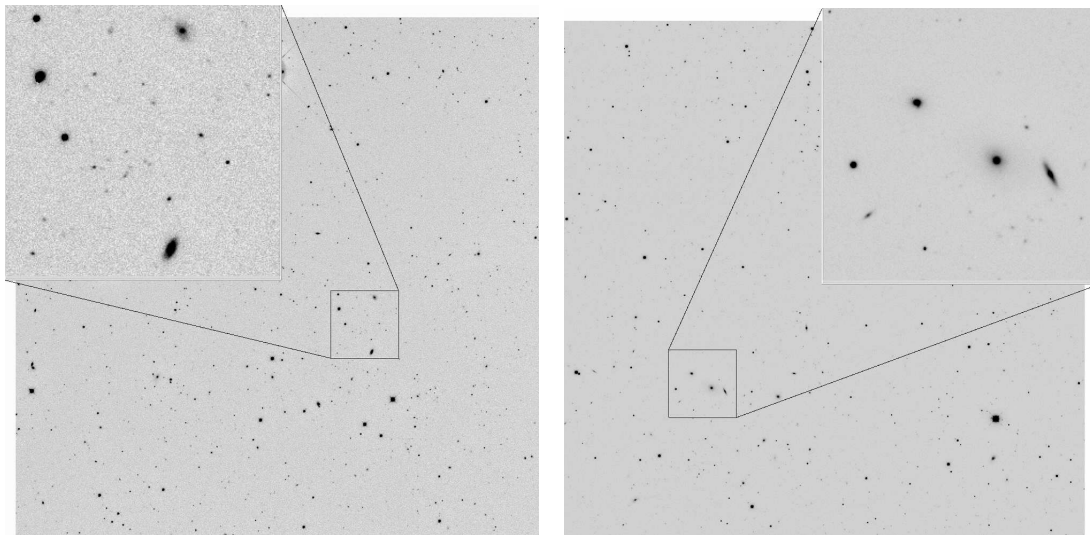

Figure 10. Science images taken in H band (left) and with a narrow band filter in J band (right). The field of view is about 15x15 arcmin and the zoom factor is 4.

5. SUMMARY AND CONCLUSIONS

The new NIR wide infrared imager installed at the 3.5 telescope in Calar Alto the last year has been described and its testing and operation have also been demonstrated. The camera was tested with three different HAWAII-2 detectors (#37, #48 and #77) and their operabilities were compared with each other. The difficulties related to the reflexion of the optical system could be solved or handled properly, so they did not impede the function of the camera. The most critical problem arose in reference to the cooperation of the detectors and the readout electronics. Two of the image sensors, #37 and #77, produced frames with a slight gradient which could not be eliminated completely but the FPA #48 did not exhibit this feature and worked with our readout electronics well during the observations. The results of the last session carried out with the FPA #77 in one channel mode are still useful for scientific purpose and only the poor weather limited the observations. The quality of the data produced by the new camera at clear nights is satisfying, so Omega2000 provides new prospects for NIR wide field imaging in the near future.

REFERENCES

1. C. A. Bailer-Jones, P. Bizenberger, and C. Storz, "Achieving a wide field infrared camera for the Calar Alto 3.5m telescope," in *Optical and IR Telescope Instrumentation and Detectors*, M. Iye and A. F. Moorwood, eds., *Proc. SPIE* **4008**, pp. 1305–1316, 2000.

2. H. Baumeister, P. Bizenberger, C. A. Bailer-Jones, Z. Kovács, H.-J. Röser, and R.-R. Rohloff, "Cryogenic engineering for Omega 2000: Design and performance," in *Instrument Design and Performance for Optical/Infrared Ground-based Telescopes*, *Proc. SPIE* **4842**, pp. 343–354, 2002.

3. K. Hodapp, "Near-infrared detector arrays: Current state of the art," in *Optical and IR Telescope Instrumentation and Detectors*, M. Iye and A. F. Moorwood, eds., *Proc. SPIE* **4008**, pp. 1228–1239, 2000.

4. K. Hodapp, D. H. J.L. Hora, L. Cowie, M. Metzger, E. Irwin, T. Keller, K. Vural, L. Kozlowski, and W. Kleinhans, "Astronomical characterization results of 1024x1024 HgCdTe HAWAII detector arrays," in *Infrared Detectors and Instrumentation for Astronomy*, A. M. Fowler, ed., *Proc. SPIE* **2475**, pp. 8–14, 1995.